THERMODYNAMICS-BASED COMPUTATIONAL APPROACH TO Al-Cu ALLOYS: GRAIN REFINEMENT

J.H. Li[1*], C. Promer[2], A. Jahn[2], B. Oberdorfer[2], S. Wurster[3], F. Martin[4], P. Schumacher[1, 2]

[1*] Chair of Casting Research, Department of Metallurgy, University of Leoben, A-8700, Leoben, Austria (jie-hua.li@hotmail.com)
[2] Austrian Foundry Research Institute, Parkstrasse 21, Leoben, Styria, A-8700, Austria
[3] Department of Materials Physics, University of Leoben, A-8700, Leoben, Austria
[4] Department of Physical Metallurgy and Materials Testing, University of Leoben, A-8700, Leoben, Austria

Abstract

To describe the solute effect on grain refinement, the growth restriction factor (Q) in multicomponent multiphase Al alloys has been often evaluated using a simple summation of the Q values of the individual constituents taken from the binary alloy diagram. Such kind of evaluation can lead to mistakes, or completely fail when an intermetallic phase, even in a trace amount, solidifies prior to the primary α-Al. A more accurate method to evaluate growth restriction factor (Q_{true}) from thermodynamic descriptions is to calculate the initial slope in the development of constitutional supercooling (ΔT) with the phase fraction of the growing solid phase (f_s). In this contribution, ThermoCalc software (with TTAl5 database) was used to evaluate the Q_{true} in a series of Al-Cu based alloys with Ti, Zr and Sc additions. This investigation demonstrates that thermodynamic-based alloy design can provide a significant tool to develop novel Al alloys.

Introduction

Al-Cu based alloys have been widely used in the automotive and aerospace industry due to their high yield strength and good fatigue resistance. However, their large freezing ranges lead to a high hot tearing tendency when compared to Al-Si based alloys. Grain refinement of Al-Cu based alloys can improve their castability, in particular improving hot tearing. However, there is still a debate on the nucleation and subsequent mechanisms for grain refinement.

Grain refinement of Al alloy has been extensively investigated for several decades both in industry and in academic, not only for developing efficient grain refiners, but also for achieving a better understanding of the grain refinement mechanism[1-12]. During grain refining of Al alloys, Al-Ti-B grain refiners have been widely investigated, due to their higher nucleation potency and wider industrial application. Various theories regarding the grain refinement mechanisms of Al-Ti-B refiners, such as the particle theory, the phase diagram theory, the duplet nucleation theory, the peritectic bulk theory, have been proposed and reviewed in [1]. Recently, the free growth theory[1-5], and modified free growth theory[6] have also been proposed. Despite of the difference between these theories, it is generally accepted that Ti has a multiple role within the melt. Firstly, Ti provides a substrate in the form of TiB_2. Secondly, excess Ti provides an enriched Ti region leading to the formation of an Al_3Ti monolayer necessary for the nucleation of Al on the stable boride substrates (TiB_2)[9-12]. Thirdly, excess Ti provides an effective growth

restriction factor (Q)[3, 4, 6, 7]. In other words, the presence of excess Ti affects both the heterogeneous nucleation and growth of Al alloys. The combined effects of enhanced copious potent nuclei and growth restriction result in the formation of desirable, small, uniform, equiaxed Al grains.

The growth restriction factor (Q) is proportional to the constitutional undercooling at the dendrite tip and can directly be used as a criterion for the grain refinement in Al alloys with strong potential nucleation particles. To describe the solute effect on grain refinement, the growth restriction factor (Q) in multicomponent multiphase alloys has often been evaluated using a simple summation of the Q values of the individual constituents taken from the binary alloy diagram. The evaluated Q is denoted as Q_{sum}. Such kind of evaluation can lead to mistakes, or completely fail when an intermetallic phase (e.g. Al_3Zr, Al_3Ti), even in trace amounts, solidify prior to the primary Al matrix[13,14]. Another method to evaluate growth restriction factor (Q) is a quasi-binary equivalent method[15]. The evaluated Q is denoted as Q_{Eq}. Although both methods have been validated, a more accurate method to evaluate growth restriction factor (Q) is to calculate the initial slope in the development of constitutional supercooling (ΔT) with the phase fraction of the growing solid phase (f_s) from thermodynamic descriptions[14, 16]. The evaluated Q is denoted as Q_{true}.

In this contribution, ThermoCalc software (with TTAl5 database) was used to evaluate the Q_{true} in a series of Al-Cu based alloys with Ti, Zr and Sc additions. The evaluated Q_{true} was compared with the evaluated Q_{sum} and Q_{Eq} using other two different methods. This investigation demonstrates that thermodynamic-based alloy design can provide a significant tool to develop novel Al alloys.

Experimental material and procedures

A series of Al-4.0Cu based alloys (wt. %, used throughout the paper, in case not specified otherwise) with Ti, Zr and Sc additions were prepared using commercial purity Al ingots (99.7), an Al-25 Cu master alloy pre-prepared in induction melting using high purity Al (99.998) and high purity Cu (99.999), and Al-10Ti, Al-10Zr, Al-2.2Sc master alloys, respectively. The nominal compositions are listed in Table I. It should be noted here that some trace elements (i.e. Fe, Mn and Si) are also present in Al-4.0Cu based alloys. However, these elements are not included for ThermoCalc calculations. ThermoCalc calculations (non-equilibrium (Scheil)) were performed to evaluate Q_{true}.

Each batch, weighting about 6 kg, was melted in a resistance furnace at 720 °C. A reference sample was taken from the melt in order to identify the grain size before inoculation. The nucleant particles (TiB_2) were added using commercial grain refiner rod (Al-5.0Ti-1.0B). The concentration of the nucleant particles (TiB_2) is about 0.01 wt % (100 ppm).

The melt was stirred with a graphite rod for 20 s after inoculation. The samples were taken from the melt at 5 min after the grain refiner addition and tested using a standard TP-1 method. The samples were sectioned 38 mm from the bottom surface. Standard metallographic procedures were performed to prepare these sections for grain size measurements. The samples were etched using a mixture of 13 g boric acid, 35 g HF, 800 ml H_2O at a voltage of 20 V for 45 seconds. All images used for grain size measurement were taken from the centre of the samples using optical microscopy in a polarized mode at the same magnification. The reported grain sizes were measured from at least 20 images using line-intersect method.

Table I: The nominal composition of a series of Al-4.0Cu based alloys with Ti, Zr, and Sc additions. (*: free Ti; #: total Zr)

Alloy No.	Cu	Si	Fe	Mn	Ti*	Zr#	Sc	Al
1	4.0	-	-	-	-	-	-	Bal.
2	4.0	-	-	-	0.1	-	-	Bal.
3	4.0	-	-	-	0.2	-	-	Bal.
4	4.0	-	-	-	-	0.25	-	Bal.
5	4.0	-	-	-	-	0.5	-	Bal.
6	4.0	-	-	-	-	-	0.25	Bal.
7	4.0	-	-	-	-	-	0.5	Bal.
8	4.0	-	-	-	-	0.25	0.25	Bal.
9	4.0	-	-	-	0.1	-	0.25	Bal.
10	4.0	-	-	-	0.1	0.25	-	Bal.

Results

ThermoCalc calculation Al-4.0Cu based alloys with Ti, Zr and Sc additions

Growth restriction factor (Q) can be evaluated using a simple summation of the Q values of the individual constituents taken from the binary alloy diagram, as listed in equation 1.

$$Q_{sum} = \sum_i m_i c_0^i (k_i - 1) \qquad (1)$$

where, for each element i, m is the liquidus gradient, c_0 is the composition, and k is the binary partition coefficient. The relative data for determining Q is listed in Table II.

Table II: Phase diagram data for determining Q in binary Al alloys[15].

Element	k	m	Max. conc. (wt.%)	m(k-1)
Cu	0.17	-3.4	33.2	2.8
Ti	7-8	33.3	0.15	~220
Zr	2.5	4.5	0.11	6.8
Si	0.11	-6.6	~12.6	5.9
Cr	2.0	3.5	~0.4	3.5
Ni	0.007	-3.3	~6	3.3
Mg	0.51	-6.2	~3.4	3.0
Fe	0.02	-3.0	~1.8	2.9
Mn	0.94	-1.6	1.9	0.1
Sc	0.64	-9.1	0.55	3.3

Growth restriction factor (Q) can be also evaluated using a quasi-binary equivalent method [15], as listed in equation 2, for Al-Si based alloys.

$$Si_{Eq} = Si + \sum Si_{Eq}^{x_i} [wt\%] \qquad (2)$$

where, equivalent is calculated as the sum of the contribution of the individual elements. For additional element (X_i, e.g. Cu, Ti), $Si_{Eq}^{X_i}$ can be determined using a mathematical model (equation 3).

$$X_{Eq}^i = a_0^{X_i} + b_0^{X_i} X_i + c_0^{X_i} X_i^2 \tag{3}$$

where, $a_0^{X_i}$, $b_0^{X_i}$, $c_0^{X_i}$ are the polynomial coefficients, respectively, as listed in Table III, X_i is the concentration of the elements (wt.%). However, it should be noted that the coefficients listed in Table III were validated in Al-Si based alloys. For Al-Cu based alloys investigated here, the coefficients may not be valid, and should be determined in an Al-Cu system, thus questioning the validation of this approach.

Inserting values calculated from equation 2 into equation 1, the Q_{Eq} values for Alloys 1-3 are determined. Due to a lack of the polynomial coefficients of Zr and Sc, no attempt was taken here to evaluate the Q_{Eq} values for Alloys 4-10.

Table III: Polynomial coefficients for various binary Al-X_i alloys representing the most common major and minor element of the Al-Si based alloys. $a_0 = 0$ for the elements presented in this table[15].

Element	b_0	c_0
Ti	-0.8159	0.009927
Zr	-	-
Ni	0.5644	-0.0285
Mg	0.0258	-0.0088
Fe	0.6495	0.0003
Cu	0.529	-0.027
Mn	0.8221	-0.0349

A more accurate method to evaluate growth restriction factor (Q) is to calculate the initial slope in the development of constitutional supercooling (ΔT) with the phase fraction of the growing solid phase (f_s) using equation 4.

$$Q_{true} = \frac{d\Delta T_c}{df_s}\Big|_{f_s \to 0} \tag{4}$$

where, ΔT_c is the rate of development of constitutional supercooling, and f_s is the fraction solid. For clarity, Figure 1 shows the evaluation of Q_{true} in Alloy 1 (Al-4Cu based alloy).

The determined Q values for Alloys 1-10 are listed in Table IV. When comparing the evaluated Q values using three different methods, it was found that (i) the Q value evaluated using equation 1 is very close to that evaluated using equation 4, if the primary phase is α-Al matrix, rather than Al$_3$Ti (Alloy 3) or Al$_3$Zr (Alloy 5). This indicates that equation 1 is valid, and can be used to evaluate the Q value in dilute Al alloys. (ii) equation 2 is not valid when Ti is present, indicating that a re-evaluation of the coefficients is required in Al-Cu based alloys. (iii) In the case of Ti and Zr addition, the Q value evaluated using equation 4 (24.2) is much less than that evaluated using equation 1 (32.9). (iv) In the case of the addition of Sc (Alloys 6, 7) and Zr (Alloys 4, 5), the evaluated Q_{true} value is very close despite of higher concentrations of each

element, indicating that an asymmetric Q values is obtained once an primary intermetallic is formed. This is not the case for Q_{sum}.
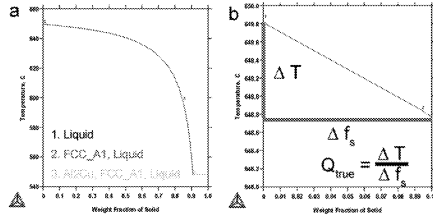

Figure 1 ThermoCalc calculation (a), and the evaluation of Q_{true} (b) in Alloy 1 (Al-4Cu based alloy). The primary phase is FCC_A1 (α-Al) solidified from liquid. Eutectic Al$_2$Cu forms subsequently.

Table IV: Comparison of Q values determined using equation 1, equation 2 and equation 4.

	Equation 1 (Q_{sum})	Equation 2 (Q_{Eq})	Equation 4 (Q_{true})
Alloy 1	11.2	9.9356	10
Alloy 2	33.2	17.93	34
Alloy 3	44.2*	7.09	35
Alloy 4	12.9	-	11.3
Alloy 5	14.6	-	11.8
Alloy 6	12.03	-	11
Alloy 7	12.85	-	11.1
Alloy 8	13.73	-	11.6
Alloy 9	34.03	-	32.6
Alloy 10	32.9	-	24.2

*Note: For Alloy 3, Q_{sum} value (44.2) was evaluated using 0.15 Ti, although 0.2 Ti was added.

Experimental investigation on Al-4.0Cu based alloys with Ti, Zr and Sc additions

Figure 2 shows a typical as-cast microstructure of Alloy 1 (Al-4Cu based alloy). The grain size is very large, about 705 ± 68 μm. The addition of TiB$_2$ (100 ppm) and excess Ti (0.1, Alloy 2) greatly decreases the grain size to 70 ± 5 μm, as shown in Figure 3. However, further increasing excess Ti (0.2, Alloy 3) results in a slight increase of grain size (80 ± 4 μm) due to the formation of primary Al$_3$Ti phase prior to α-Al phase (not shown here).
The addition of Zr (0.25, Alloy 4) does not greatly decrease the grain size. The grain size is about 142 ± 13 μm (Figure 4). Further increasing the Zr content (0.5, Alloy 5) does not result in a decrease in grain size. The grain size is about 131 ± 10 μm (Figure 5).
The addition of hypoeutectic Sc (0.25, Alloy 6) does not greatly decrease the grain size. The grain size is about 282 ± 44 μm (Figure 6), much higher than that (142 ± 13 μm) with 0.25 Zr addition (Figure 5). This can be attributed to the higher solute solubility of Sc compared with Zr in Al (Table II). At the same addition level (e.g. 0.25), no significant fraction of primary Al$_3$Sc phase form as nucleation sites for α-Al. Further increasing Sc (0.5, Alloy 7) decrease the grain

size by additional Q but remains hypoeutectic (less than 0.55, Table II). The grain size is about 140 ± 8 μm. However, the combined addition of Zr and Sc (Alloy 8) greatly decrease the grain size. The grain size is about 110 ± 10 μm (Figure 7).
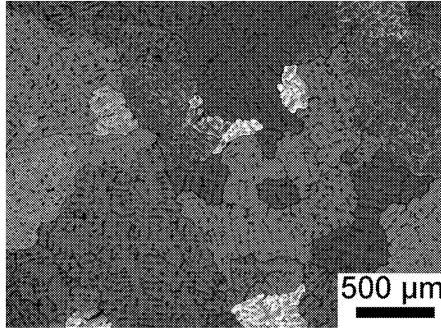

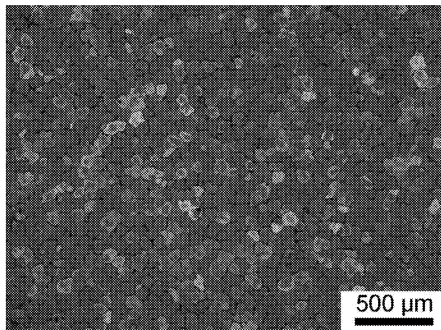Figure 2 As-cast microstructure of Alloy 1 (Al-4Cu based alloy). The grain size is about 705 ± 68 μm.

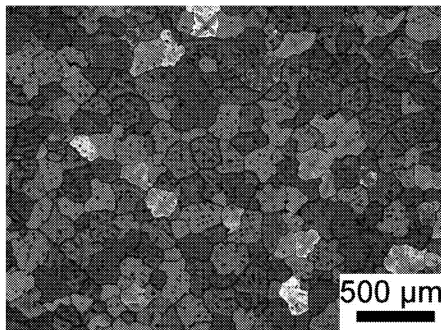Figure 3 As-cast microstructure of Alloy 2 (with 0.1 Ti addition).   The grain size is about 70 ± 5 μm.

Figure 4 As-cast microstructure of Alloy 4 (with 0.25 Zr). The grain size is about 142 ± 13 μm.
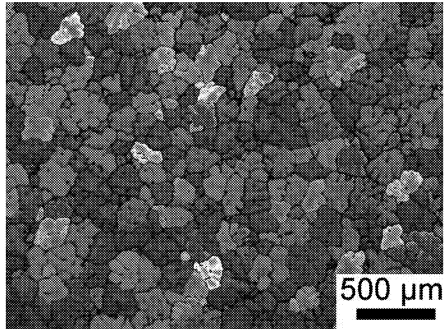
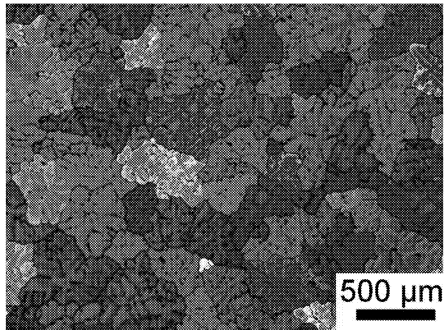Figure 5 As-cast microstructure of Alloy 5 (with 0.5 Zr addition). The grain size is about 131 ± 10 μm.

Figure 6 As-cast microstructure of Alloy 6 (with 0.25 Sc addition). The grain size is about 282 ± 44 μm.
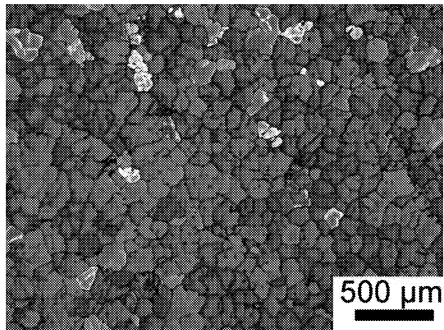

Figure 7 As-cast microstructure of Alloy 8 (with 0.25 Zr and 0.25 Sc). The grain size is about 110 ± 10 μm.

Discussions

The Q values (Table IV) evaluated using equation 1 and equation 4 can be used to interpret the change of grain size (Figures 2-7) observed using TP-1 test. For example, in the case of Ti addition, the presence of excess Ti (0.1, Alloy 2) increases growth restriction factor (Q) sharply (Table IV) from 10 (Alloy 1) to 34 (Alloy 2). A higher growth restriction factor (Q) leads to a significant decrease of the grain size from 705 ± 68 µm (Figure 1) to 70 ± 5 µm (Figure 3, as shown in Figure 8, which is similar to cases of TiB$_2$ addition in Al alloys. This strongly indicates that the evaluation of growth restriction factor using equation 1 (Q_{sum}) and equation 4 (Q_{true}) is reliable.

Comparing the Q_{true} and Q_{sum} values for Alloy 2 and Alloy 3, it is apparent that only Q_{true} predicts for the identical cooling condition. Similar grain size is obtained for Alloy 2 (70 ± 5 µm) and Alloy 3 (80 ± 4 µm). Similarly, Q_{true} also predicts similar grain size for Alloy 4 (142 ± 13 µm) and Alloy 5 (131 ± 10 µm). Overall, Q_{true} gives a better evaluation of growth restriction factor.
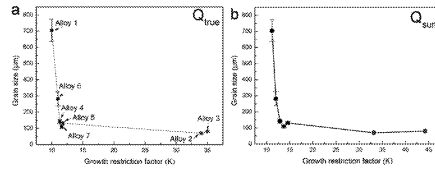

Figure 8 Grain size decreases with growth restriction factor increasing.

In the case of Zr and / or Sc addition, the evaluated growth restriction factor (Q_{sum} and Q_{true}) is nearly the same (about 11, Table IV, Alloys 6-8). However, the grain size changes greatly, especially for a combined addition of Zr and Sc (Figure 7). One important question arises, why the grain size changes greatly even with the same growth restriction factor. Is growth restriction factor a dominant factor affecting the grain refinement, or should any other mechanisms (i.e. heterogeneous nucleation and interactions between solutes) also be taken into consideration ?

A strong interaction between solutes, i.e. forming the τ phase during solidification, has been reported that Al-Si-Ti ternary alloys[13]. This interaction affects the evaluation of growth restriction factor. However, unlike Al-Si-Ti systems, Al-4.0Cu based alloys do not exhibit a strong interaction between solutes (i.e. Cu, Ti), because no Cu-rich phase forms during solidification.

The reported Zr-poisoning between TiB$_2$ and Zr[17] suggests that an interaction between TiB$_2$ and Zr to forming ZrB$_2$, which does not act as a good nucleation site. However, here no TiB$_2$ is present, and above the composition for the onset of the peritectic reaction (0.11, Table II), Al$_3$Zr is formed acting as nucleation site and the remaining Zr as a poor growth restrictor. This hypothesis can be further supported by the lower evaluated growth restriction factor (Q) (Table IV, Alloy 10).

The interaction between solutes definitely affects the heterogeneous nucleation of α-Al, i.e. enhancing or deactivating the nucleation potency. In the case of Ti addition, the presence of excess Ti and thus the possible formation of Ti-rich layers will reduce the growth velocity of the nucleated crystals and increase the maximum undercooling achievable before recalescence[7]. This allows more particles to be active in nucleation and, consequently, increases the number

density of the active particles, giving rise to a finer grain size. In the case of combined addition of Zr and Sc, three aspects should be taken into consideration. Firstly, the formation of Al$_3$(Zr, Sc) reduces the lattice parameter of both the stable DO$_{23}$ and metastable L1$_2$ Al$_3$Zr, thus decreases the mismatch between the nucleation sites particles and α-Al matrix (Table V), and finally promotes the nucleation of α-Al[18,19]. Secondly, the combined addition of Zr and Sc reduces the solute solubility of each other[18]. More nucleating sites are available for the nucleation of α-Al. Thirdly, in the case of single Sc addition, most Al$_3$Sc (if any, once Sc content is above 0.55) formed through an eutectic reaction will be pushed to the grain boundaries, while in the case of the combined Zr and Sc addition, a so-called shell-core Al$_3$(Zr, Sc) formed through a eutectic reaction, will be surrounded by α-Al, as a good nucleation site. For clarity, a schematic diagram is shown in Figure 9. Some typical SEM images taken from Alloy 5 (0.5 Zr) and Alloy 8 (0.25 Zr and 0.25 Sc) are shown in Figure 10. Clearly, in the case of a single Zr addition (0.5), an Al$_3$Zr particle was located at the center of the grain, and acted as a nucleation site (Figure 10a). In the case of combined additions of Sc and Zr, Al$_3$(Zr, Sc) forms during solidification. Al$_3$Zr solidified as a core and was covered by an Al$_3$Sc shell (Figure 10c).

Table V: Lattice parameters and mismatch between the particles and Al matrix[18].

Particles	Lattice parameters (nm)	Mismatch	Orientation ship
Al$_3$Ti	DO22 a = 0.3851 c = 0.8608	0.23	(221)$_{Al}$ // (011)$_{Al3Ti}$, [110]$_{Al}$ // [210]$_{Al3Ti}$
Al$_3$Zr	DO23, L1$_2$ a = 0.4048	0.8	Any plane and directions
Al$_3$Sc	L1$_2$ a = 0.4105	< 1.5 (1.2)	Any plane and directions

The diffusion of solute elements (i.e. Ti, Sc, Zr and Cu) should also be taken into consideration when discussing the grain refinement of Al alloys. The partition behaviour of Ti (k = 7-8 in pure Al) is much stronger than that of Cu (k = 0.17), Zr (k = 2.5) and Sc (k = 0.64). It can be expected that Ti partitions more easily into the nucleants than Cu, thus forming a Ti-rich region. The possible formation of a Ti-rich region will affect the interface structure (i.e. ordering or disordering)[20], reducing the interface energy, and thus reducing the required undercooling for nucleation[1]. Then, smaller nucleants can be activated. This suggestion is fully consistent with a modified free growth model[6], which suggests that the nucleation potency of inoculation particles is reduced by the solute field (Ti-rich region) that develops close to existing, growing equiaxed grains under near isothermal conditions. Solute suppressed nucleation leads to much lower nucleated grain densities, higher nucleation undercooling and longer times to recalescence when further nucleation events are halted. Thus, it can be concluded that activating more nucleants, rather than growth restriction factor (Q), is the key factor for grain refinement. In other words, a high growth restriction factor is necessary for nucleants to be activated, but the enhanced heterogeneous nucleation is the dominant factor for grain refinement of Al alloys. In foundry practices, attempts should be made to enhance the heterogeneous nucleation of α-Al, and thus to achieve a desirable, small, uniform, equiaxed Al grains.
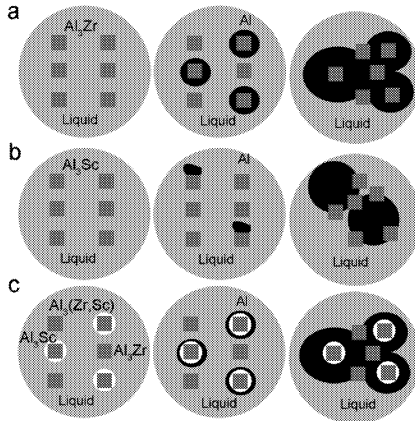
Figure 9 Schematic diagram showing (a) peritectic reaction for Zr addition (higher than 0.11), (b) eutectic reaction for Sc addition (higher than 0.55), and (c) eutectic reaction for Zr and Sc addition.
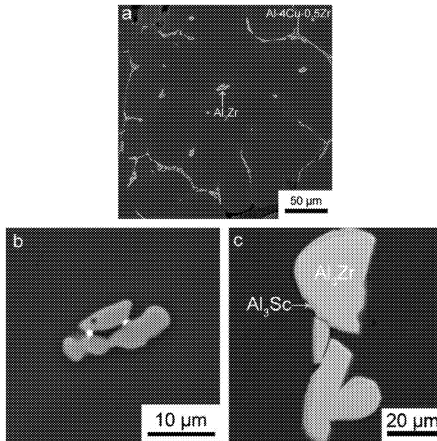

Figure 10 SEM images taken from Alloy 5 (0.5 Zr) and Alloy 8 (0.25 Zr and 0.25 Sc), showing an Al_3Zr particle was located at the center of the grain (a,b) in the case of Zr (0.5) addition, and another Al_3Zr was covered by an Al_3Sc shell (c) in the case of Zr (0.25) and Sc (0.25) addition.

Conclusion

1.   In Al-Cu based alloy, the evaluated Q_{sum} and Q_{true} values are nearly identical due to low interaction between the alloying constituents.

2.   A more accurate method to evaluate growth restriction factor is to calculate the Q_{true} using equation 4 at complex alloy systems. Under identical cooling condition in the TP-1 test, Q_{true} predicts grain size more accurately than Q_{sum}.

3.   For dilute Al alloy, the evaluated Q values can be used to interpret the change of grain size observed using TP-1 test.

4.   More attention should be paid when the summation of Q values of the individual constituents taken from the binary alloy diagram is used to evaluate growth restriction factor (Q) because a mistake or a complete fail may occur when α-Al is not the primary phase.

5.   The presence of excess Ti results in an enhanced grain refinement due to increased growth restriction factor and enhanced heterogeneous nucleation.

6.   The combined Zr and Sc additions enhanced the heterogeneous nucleation, and thus resulting in an enhanced grain refinement, although the growth restriction factor remained unchanged.

7.   Heterogeneous nucleation is a dominant factor for grain refinement of Al alloys.

References

[1]   A.L. Greer, A.M. Bunn, A. Tronche, P.V. Evans, D.J. Bristow. Acta Mater., 48 (2000) 2823-2835.
[2]   T.E. Quested, A.L. Greer. Acta Mater., 52 (2004) 3859-3868.
[3]   T.E. Quested, A.L. Greer. Acta Mater., 53 (2005) 4643-4653.
[4]   T.E. Quested, A.T. Dinsdale, A.L. Greer. Acta Mater., 53 (2005) 1323-1334.
[5]   T.E. Quested, A.L. Greer. Acta Mater., 53 (2005) 2683-2692.
[6]   D. Shu, B.D. Sun, J. Mi, P.S. Grant. Acta Mater., 59 (2011) 2135-2144.
[7]   H. Men, Z. Fan. Acta Mater. 59 (2011): 2704-2712.
[8]   H.T. Li, M. Xia, Ph. Jarry, G.M. Scamans, Z. Fan. Journal of Crystal Growth. 314 (2011) 285-292.
[9]   P. Schumacher, A.L. Greer. Mater. Sci. Eng. A, 181-182 (1994): 1335-1339.
[10] N. Iqbal, N.H. van Dijk, T. Hansen, L. Katgerman, G.J. Kearley. Mater. Sci. Eng. A, 386 (2004): 20-26.
[11] N. Iqbal, N.H. van Dijk, S.E. Offerman, N. Geerlofs, M.P. Moret, L. Katgerman, G.J. Kearley. Mater. Sci. Eng. A, 416 (2006): 18-32.
[12] N. Iqbal, N.H. van Dijk, S.E. Offerman, M.P. Moret, L. Katgerman, G.J. Kearley. Acta Mater., 53 (2005): 2875-2880.
[13] J. Gröbner, D. Mirković, R. Schmid-Fetzer. Mater. Sci. Eng. A, 395 (2005): 10-21.
[14] R. Schmid-Fetzer, A. Kozlov. Acta Mater. 59 (2011): 6133-6144.
[15] A.M. Mitrašinović, F.C. Robles Hernández. Mater. Sci. Eng. A, 540 (2012): 63-69.
[16] G.N. Haidemenopoulos, A.I. Kastsamas, H. Kamoutsi. Metall. Mater. Trans. A., 41 (2010) 888-899.
[17] A.M. Bunn, P. Schumacher, M.A. Kearns, C.B. Boothroyd, A.L. Greer. Mater. Sci. Tech., 15 (1999): 1115-1123.
[18] C. Booth-Morrison, Z. Mao, M. Diaz, D.C. Dunand, C. Wolverton, D.N. Seidman. Acta Mater. 60 (2012): 4740-4752.
[19] O. Beeri, D.C. Dunand, D.N. Seidman. Mater. Sci. Eng. A, 527 (2010): 3501-3509.
[20] J.S. Wang, A. Horsfield, P.D. Lee, P. Brommer. Phys. Rev. B, 82 (2010) 144203.